



Published in final edited form as:

*J Glaucoma*. 2018 June ; 27(6): 481–489. doi:10.1097/IJG.0000000000000964.

## Optical Coherence Tomography Angiography Macular Vascular Density Measurements and the Central 10-2 Visual Field in Glaucoma

Rafaella C. Penteadó, MD<sup>1</sup>, Linda M. Zangwill, PhD<sup>1</sup>, Fábio B. Daga, MD<sup>1</sup>, Luke J. Saunders, PhD<sup>1</sup>, Patricia Isabel C. Manalastas, MD<sup>1</sup>, Takuhei Shoji, MD, PhD<sup>1,2</sup>, Tadamichi Akagi, MD, PhD<sup>1,3</sup>, Mark Christopher, PhD<sup>1</sup>, Adeleh Yarmohammadi, MD<sup>1</sup>, Sasan Moghimi, MD<sup>1</sup>, and Robert N. Weinreb, MD<sup>1</sup>

<sup>1</sup>Hamilton Glaucoma Center, Shiley Eye Institute, Department of Ophthalmology, University of California San Diego, La Jolla, CA

<sup>2</sup>Saitama Medical University, Saitama, Japan

<sup>3</sup>Department of Ophthalmology and Visual Sciences, Kyoto University Graduate School of Medicine, Kyoto, Japan

### Abstract

**Purpose**—To evaluate the association between macula vascular density assessed by optical coherence tomography angiography (OCT-A) and central visual field (VF) threshold sensitivities in healthy, glaucoma suspect and glaucoma patients.

**Methods**—A total of 185 eyes from 38 healthy participants, 31 glaucoma suspects, 72 mild glaucoma patients, and 44 moderate/severe glaucoma patients from the Diagnostic Innovations in Glaucoma Study who underwent OCT-A images of the macula and 10-2 VF testing were enrolled in this observational cross-sectional study. The relationship between central VF mean sensitivity and superficial macula whole-image vessel density (wiVD), and the relationship between the MS of the four central points of the 10-2 VF (MS4) and parafoveal vessel density (pfVD), were assessed using linear regression models.

**Results**—Mean wiVD (52.5%, 49.8%, 49.4% and 45.2%, respectively) and mean pfVD (54.9%, 52.1%, 51.8% and 47.7%, respectively) were found to be significantly higher in healthy eyes and glaucoma suspect eyes compared to glaucoma eyes with mild and moderate/severe disease (ANCOVA  $P < 0.001$ ). The univariate associations between 10-2 mean sensitivity and wiVD ( $R^2 = 26.9\%$ ) and between 10-2 MS4 and pfVD ( $R^2 = 16.8\%$ ) were statistically significant ( $P < 0.001$  for both). After adjusting for scan quality, age, gender and intraocular pressure, superficial macula

---

Corresponding author: Robert N. Weinreb, MD, Hamilton Glaucoma Center and Department of Ophthalmology, University of California, San Diego, 9500 Gilman Drive, La Jolla, CA, 92093-0946, rweinreb@ucsd.edu.

### Disclosures

**Financial Disclosures:** Rafaella C. Penteadó: none; Linda M. Zangwill: Research support – Carl Zeiss Meditec, Heidelberg Engineering, National Eye Institute, Topcon Inc; Fabio B. Daga: none; Luke J. Saunders: none; Patricia Isabel C. Manalastas: none; Takuhei Shoji: Research support – Pfizer, Senju, Alcon, Santen, Kowa, Otsuka; Tadamichi Akagi: Research support – Santen, Pfizer, Senju, Alcon, Kowa; Mark Christopher: none; Adeleh Yarmohammadi: none; Sasan Moghimi: none; Robert N. Weinreb: Research support – Carl Zeiss Meditec, Genentech, Heidelberg Engineering, National Eye Institute, Optovue, Optos and Topcon; Consultant – Aerie Pharmaceuticals, Alcon, Allergan, Bausch & Lomb, Novartis, Sensimed, Valeant.

wiVD and pfVD were still independently associated with central VF loss. Macula wiVD performed better (AUROC=0.70) than GCC thickness (AUROC=0.50) for differentiating between glaucoma suspect and healthy eyes ( $P=0.010$ ).

**Conclusions**—Loss of OCT-A macula vessel density is associated with central 10-2 VF defects. Macula vessel density is a clinically relevant parameter that may enhance monitoring of glaucoma suspects and patients.

### Keywords

Optical coherence tomography angiography; glaucoma; macula; vessel density

---

## Introduction

Primary open angle glaucoma (POAG) is a chronic optic neuropathy characterized by progressive degeneration of retinal ganglion cells and their axons, resulting in structural damage to the optic nerve head and inner retina accompanied by irreversible visual field loss.<sup>1</sup> Approximately half of these retinal ganglion cells are located within 4.5mm of the center of the fovea. This area, particularly the inferior region known as the macula vulnerability zone, is susceptible to damage in the early stages of glaucoma.<sup>2-10</sup>

Although the pathogenesis of POAG is still unknown, it has been suggested that retinal blood flow may have a role in the development and progression of the disease.<sup>11-13</sup> Numerous imaging modalities have been used to assess the retinal microvasculature and perfusion, including fluorescein angiography. However, fluorescein angiography provides limited visualization of the retinal radial peripapillary capillary vessels and macula capillary networks. Moreover, it requires exposure to a contrast agent.<sup>14</sup> In contrast, optical coherence tomography angiography (OCT-A) provides non-invasive reproducible qualitative and quantitative evaluation of the vasculature in the macula, optic nerve head and peripapillary region.<sup>15-18</sup>

Although loss of peripapillary microvasculature and visual field damage<sup>19, 20</sup> are strongly correlated, there is still limited information regarding the relationship between the superficial macula microvasculature damage and visual function. However, structural and functional testing of the macula enhances both the diagnosis and monitoring of glaucoma.<sup>4</sup> Therefore, the purpose of this study was to evaluate the relationship of macula vascular density assessed by OCT-A and the central 10-2 visual field mean sensitivity in normal subjects, glaucoma suspects and glaucoma patients.

## Methods

Participants from the Diagnostic Innovations in Glaucoma Study (DIGS) who underwent OCT-A and visual field testing were included in this cross-sectional study. Details of the DIGS protocol and eligibility have been described previously.<sup>21</sup> All participants completed a comprehensive ophthalmological examination, including best-corrected visual acuity, slit-lamp biomicroscopy, intraocular pressure (IOP) measurement by Goldmann applanation tonometry, gonioscopy, dilated fundus examination, stereoscopic optic disc photography, and

standard automated perimetry (SAP) using the Swedish Interactive Threshold Algorithm on the Humphrey Field Analyzer (Carl Zeiss Meditec, Dublin, CA) in both eyes. Only participants with open angles on gonioscopy, and spherical refraction within  $\pm 10$  diopters were included in the study.

This study was conducted in accordance with the tenets of the Declaration of Helsinki, was approved by the Institutional Review Board at the University of California San Diego, and met the requirements of the Health Insurance Portability and Accountability Act regulations. Written informed consent was obtained from all participants.

## Participants

Healthy subjects were required to have an IOP of 21mmHg or lower without history of elevated IOP; normal-appearing optic discs, neuroretinal rims, and retinal nerve fiber layer (RNFL); and normal visual field test results, defined as pattern standard deviation (PSD) within the 95% confidence limits and glaucoma hemifield test (GHT) results within normal limits. Glaucoma suspects were defined as having elevated IOP ( $\geq 22$ mmHg) or suspicious-appearing optic discs without the presence of repeatable glaucomatous visual field damage.

POAG was defined as the presence of two or more repeatable abnormal SAP 24-2 results with GHT outside normal limits or PSD outside 95% normal limits. Patients with glaucoma were stratified into 2 categories based on the severity of their visual field damage. Patients with mean deviation (MD) higher than  $-6.0$  decibels (dB) were classified as Mild Glaucoma, and patients with MD equal or lower than  $-6.0$  were classified as Moderate to Severe Glaucoma.<sup>22</sup>

Participants with a history of intraocular surgery (except for uncomplicated cataract or glaucoma surgery), coexisting retinal pathologies, non-glaucomatous optic neuropathy, uveitis, or ocular trauma were excluded from the study. Only subjects with reliable tests ( $\geq 33\%$  fixation losses and false-negatives, and  $\leq 15\%$  false-positives) were included in the analysis. The quality of visual field tests was reviewed by the Visual Field Assessment Center (VisFACT).<sup>23</sup> Only tests without signs of rim and eyelid artifacts, without evidence of inattention or fatigue effects, and without abnormal results caused by diseases other than glaucoma were included.

Systemic blood pressure (BP) was measured in a seated position using the Omron Automatic (Model BP791IT; Omron Healthcare, Inc., Lake Forest, IL, USA) blood pressure monitor. Mean arterial pressure was calculated as one-third of the systolic BP plus two-thirds of the diastolic BP. Mean ocular perfusion pressure (MOPP) was defined as the difference between two-thirds of the mean arterial pressure and the IOP.<sup>24</sup>

## Standard Automated Perimetry

The 24-2 visual field results were used to classify the severity of the disease as described above. Participants also underwent 10-2 visual field testing. Threshold sensitivity values were converted from decibels (dB) to 1/Lambert values with the following formula:  $1/\text{Lambert} = 10^{\text{dB}/10}$ . The mean sensitivity (MS) of the entire 10-2 visual field was calculated as the average of the threshold sensitivity values (1/L) of all 68 points tested. The mean

sensitivities of the eight and four central points (MS8 and MS4) were calculated as the average of the threshold sensitivity values of the eight (4 points located 1 degree in each direction away from the fovea and 4 points located 3 degrees in each direction away from the fovea) and four (4 points located 1 degree in each direction away from the fovea) central points of the 10-2 visual field, respectively. These central points correspond to the whole image and parafoveal region when adjusting for retinal ganglion cell displacement (Figure 1).<sup>25, 26</sup>

### Optical Coherence Tomography Angiography

The Avanti Angiovue system (Optovue, Inc. Fremont, CA), consisting of a combined OCT-A and spectral domain optical coherence tomography (SD-OCT) system, provides non-invasive visualization of the retinal vascular network by using motion contrast technique optimized for the split-spectrum amplitude-decorrelation angiography (SSADA) algorithm described previously.<sup>27</sup> The OCT-A Angiovue analysis software automatically calculates vessel density as the percentage (%) of measured area occupied by flowing blood vessels defined as pixels having decorrelation values above the threshold level. SD-OCT and OCT-A images were acquired by the same operator in the same visit. A previous reproducibility study from our group has reported good reproducibility of macula scans acquired on 2 separate visits by different operators (intervisit Coefficient of Variation 6.1% in healthy and 4.2% in glaucoma patients).<sup>28</sup>

For this study, we analyzed vessel density from 3mm × 3mm macula scans consisting of merged Fast-X volume of 304 horizontal B-scans of 304 A-scans per B-scan and Fast-Y volume of 304 horizontal B-scans of 304 A-scans per B-scan centered on the fovea. Each scan was automatically segmented by the Angiovue software (version 2015.1.0.90) in order to visualize the superficial retinal capillary plexuses (SCP) and deep retinal capillary plexuses (DCP) of the retina. Only SCP macula vessel density, measured from 3µm below the internal limiting membrane (ILM) to 15µm below the inner plexiform layer (IPL), was used in the analysis. Measurements were obtained in two areas. Whole image vessel density (wiVD) was measured in the entire en-face 3mm × 3mm image, and parafoveal vessel density (pfVD) was measured in an annular region with an inner diameter of 1mm and an outer diameter of 3mm centered on the fovea (Figure 1).

Image quality review was performed by trained observers following a standard protocol established by the University of California, San Diego Imaging Data Evaluation and Analysis (IDEA) Reading Center.<sup>29</sup> Scans with poor quality, defined by the following criteria, were not included: (1) a signal strength index (SSI) less than 48 (1 = minimum, 100 = maximum), (2) poor clarity, (3) residual motion artifacts visible as irregular vessel pattern on the en-face angiogram, (4) local weak signal, and (5) off-centered fovea. From our reading center data, approximately 25% of the scans are excluded because of poor quality. If both eyes qualified for this study, one eye was randomly selected for analysis.

## Spectral-Domain Optical Coherence Tomography Imaging

All subjects also underwent macular cube imaging with a commercially available SD-OCT system (Avanti Angiovue) with a 70kHz axial line rate, an 840nm central wavelength, and an axial resolution of 5 $\mu$ m in tissue.

The ganglion cell complex (GCC) scanning protocol was used to measure the GCC thickness, which consists of the ganglion cell layer, inner plexiform layer and retinal nerve fiber layer. The 7mm  $\times$  7mm macular cube is centered on the fovea and is composed by 1 horizontal B-scan and 15 vertical B-scans. Each B scan comprises 933 A-scans. The area covered by the 7mm  $\times$  7mm macula scan is comparable to the area covered by the entire 10-2 visual field. Only good quality images, defined by scans with a signal strength index  $\geq$  40, and without segmentation failure and artifacts were included. The global mean GCC thickness was included in the analysis.

## Statistical Analysis

Descriptive statistics were calculated as the mean and standard deviation. Analysis of variance (ANOVA) and post-hoc Tukey honestly significant difference (HSD) test, and Analysis of Covariance (ANCOVA) were performed to compare mean values among the healthy, glaucoma suspect, mild glaucoma, and severe to moderate glaucoma eyes. Relationships between visual field mean sensitivity and vessel density, GCC thickness, and SSI were assessed using simple linear regression. Multiple linear regression model was used to evaluate the relationship between VF sensitivity and vessel density while adjusting for possible confounders. Area under the receiver operator characteristic (AUROC) curves were adjusted for age differences between groups. Pairwise comparisons of the AUROCs were performed to evaluate whether there were statistically significant differences between the ROC curves.

A *P*-value  $<0.05$  was considered statistically significant. All statistical analyses were performed with Stata software version 14 (StataCorp LP, College Station, TX).

## Results

The demographic and clinical characteristics of the 38 healthy participants, 31 glaucoma suspects, 72 mild glaucoma patients, and 44 moderate/severe glaucoma patients are presented in Table 1. Moderate to severe glaucoma patients were older and had lower IOP compared to healthy eyes and glaucoma suspects. In addition, the percentage of females was smaller among the moderate/severe glaucoma patients than in the healthy participants. Race and MOPP were not significantly different among groups (ANOVA *P*=0.302 and *P*=0.949, respectively).

Moderate to severe glaucoma eyes generally had sparser macula capillary networks compared to healthy eyes, glaucoma suspects or mild glaucoma eyes. The average wiVD for healthy eyes, glaucoma suspects, mild glaucoma patients, and moderate/severe glaucoma patients was  $52.5 \pm 3.7$  %,  $49.8 \pm 3.7$  %,  $49.4 \pm 3.9$  % and  $45.2 \pm 3.9$  %, respectively. The mean pfVD for the groups were  $54.9 \pm 3.7$  %,  $52.1 \pm 3.7$  %,  $51.8 \pm 4.1$  % and  $47.7 \pm 4.5$  %, respectively (Table 1). After adjusting for age, both wiVD and pfVD were found to be

significantly different between groups (ANCOVA  $P<0.001$ ), with  $P<0.05$  for all pairwise comparisons except between glaucoma suspects and mild glaucoma patients ( $P=0.782$  for wiVD and  $P=0.705$  for pfVD).

Average GCC thickness values for healthy eyes, glaucoma suspects, mild glaucoma patients, and moderate/severe glaucoma patients were  $93.9 \pm 8.0 \mu\text{m}$ ,  $93.2 \pm 10.7 \mu\text{m}$ ,  $83.6 \pm 10.1 \mu\text{m}$  and  $72.5 \pm 12.2 \mu\text{m}$ , respectively. These measurements were found to be significantly different between groups after adjusting for age (ANCOVA  $P<0.001$ ) and in all pairwise comparisons except between healthy and glaucoma suspect eyes ( $P=0.874$ ).

Of the univariable linear models fitted, the relationship between the 10-2 visual field MS (1/L) and GCC had the strongest association ( $R^2=32.76\%$ ), followed by the relationship between MS (1/L) and OCT-A wiVD ( $R^2=26.94\%$ ), the relationship between MS8 (1/L) and OCT-A wiVD ( $R^2=22.74\%$ ) and the association between MS4 and pfVD ( $R^2=16.85\%$ ); all 4 associations were statistically significant ( $P<0.001$ ) (Figure 2). After adjusting for age, these associations were found to be even stronger ( $R^2=41.75\%$ ,  $R^2=30.76\%$ ,  $R^2=27.04\%$ ,  $R^2=20.62\%$ , respectively).

Area under the receiver operator characteristic (AUROC) curves were calculated for OCT-A wiVD and SD-OCT GCC thickness (Figure 3). The age-adjusted AUROC of GCC thickness (0.863) was higher than the AUROC of wiVD (0.757) ( $P=0.011$ ) for differentiating between glaucoma and healthy eyes. Conversely, macula wiVD performed better (AUROC=0.705) than GCC thickness (AUROC=0.506) for differentiating between glaucoma suspect and healthy eyes ( $P=0.010$ ).

Age-adjusted OCT-A SSI was statistically different among diagnostic groups (ANCOVA  $P<0.001$ ), with significant differences in SSI found in post-hoc analysis between healthy and glaucoma suspects, healthy and moderate to severe glaucoma, and mild glaucoma and moderate to severe glaucoma (Table 1); other comparisons did not reach statistical significance. SD-OCT values were significantly higher in healthy eyes compared to glaucoma suspects, mild glaucoma patients and moderate to severe glaucoma patients after adjusting for age (ANCOVA  $P<0.001$ ). After adjusting for age, the associations between OCT-A SSI and wiVD and pfVD were found to be  $R^2=55.1\%$  and  $R^2=54.8\%$ , respectively ( $P<0.001$  for both). All pairwise comparisons of SD-OCT SSI by diagnostic group except between glaucoma suspects and mild glaucoma ( $P=0.998$ ) were statistically different ( $P<0.05$ ) from one another (Table 1). OCT-A SSI was linearly associated with wiVD and pfVD ( $R^2=53.2\%$  and  $R^2=52.6\%$ , respectively,  $P<0.001$  for both). A weaker but also statistically significant association was found between SD-OCT SSI and GCC thickness ( $R^2=7.85\%$ ,  $P<0.001$ ), which became stronger after adjusting for age ( $R^2=22.32\%$ ,  $P<0.001$ ).

Because significant differences in age, gender, IOP and SSI were found among diagnostic groups, these variables were included in multivariable analyses. After controlling for these variables in multivariable analysis independent associations between MS and wiVD, MS8 and wiVD, and MS and GCC thickness were found. OCT-A SSI was not a significant predictor of MS, MS8 or MS4 when wiVD or pfVD were included in the model as



covariates (Tables 2 to 5). In contrast, SD-OCT SSI was independently associated with GCC thickness and 10-2 MS (Table 5).

## Discussion

In this study, it was found that superficial macula whole-image and parafoveal vessel densities (assessed by OCT-A) and GCC thickness (assessed by SD-OCT) were lower in patients with moderate to severe glaucoma when compared to healthy subjects, glaucoma suspects or patients with mild glaucoma. Moreover, macula vessel density was significantly associated with 10-2 visual field sensitivity, and their measurements were also significantly associated with the quality of the scan in univariable analysis.

The application of OCT-A for the study of vasculature in glaucomatous eyes largely has focused on the radial peripapillary capillaries around the optic nerve head.<sup>16, 19, 29–39</sup> We have previously reported a relatively strong relationship between optic nerve head wiVD and the MS of the 24-2 VF ( $R^2=44\%$ ).<sup>19</sup> It should be noted that the peripapillary region is supplied by the superficial vascular plexus (ganglion cell layer and inner plexiform layer) and the radial peripapillary capillary plexus (nourishment of the nerve fiber layer).<sup>40</sup> For the current study, we evaluated macular vascular information from the superficial capillary plexus, i.e. blood vessels located within a volume between the nerve fiber layer (NFL) and the inner plexiform layer. The superficial capillaries mainly nourish the ganglion cell layer, the nerve fiber layer and other inner layers.<sup>41</sup> However, this superficial vascular plexus anastomoses freely with the deep vascular plexus, resulting in a complex vascular supply network for the macula.<sup>42</sup>

OCT-A macula vessel density in normal eyes and in eyes with various ophthalmic pathologies previously has been investigated.<sup>17, 18, 43–54</sup> Other studies using Angiovue 3mm × 3mm macula OCT-A scans in healthy eyes reported mean superficial wiVD of 52.58%<sup>45</sup> and 51.39%<sup>46</sup>, and superficial pfVD values of 46.96%<sup>17</sup> (median) and 53.62%<sup>47</sup> (mean), which are in agreement with the current results that showed wiVD of 52.52% and pfVD of 54.86% for normal eyes. In contrast, another study using 3mm × 3mm OCT-A scans obtained with a different device found lower wiVD (31.68%) in normal subjects.<sup>48</sup> Since thickness measurements obtained by different OCT devices are not interchangeable,<sup>55, 56</sup> these discrepant findings are likely be a result of using different instruments. Estimates of superficial retinal layer vascular density of the perifoveal region of healthy post-mortem eyes have been reported to be between 31% and 55%.<sup>57</sup>

Our results confirm previous findings that severe glaucoma subjects had significantly lower macula vessel density values compared to early glaucoma or healthy eyes.<sup>58</sup> Xu and colleagues also found a positive correlation between wiVD of the superficial and deep retinal layers combined and 10-2 MS.<sup>58</sup> Their study, however, did not include glaucoma suspects and we are unaware of other studies assessing the relationship between macula vessel density and central visual field mean sensitivity in glaucoma suspects. In addition, we found that both wiVD and pfVD age-adjusted values were higher in healthy eyes compared to glaucoma suspects, and that these values were not different when comparing glaucoma suspects to mild glaucoma eyes ( $P=0.782$  and  $P=0.705$ , respectively). In contrast, age-

adjusted GCC thickness was not significantly different between healthy eyes and glaucoma suspect eyes ( $P=0.874$ ), but GCC was significantly thicker in the suspect group compared to the group with early disease. This important finding suggests that at least in some eyes the decline in the microvascular vessel density may precede the loss of retinal nerve fibers in glaucoma. Although the above mentioned results may have been influenced by the difference in size between GCC thickness and macular VD scans, thickness scan resolution and/or the exclusion of about 25% of OCT-A images due to poor quality, they are consistent with a recent longitudinal study by Shoji and colleagues that reported a more rapid loss of Angiovue-based OCT-A macula vessel density than either OCT circumpapillary retinal nerve fiber thickness or OCT ganglion cell complex thickness.<sup>59</sup> Additional longitudinal studies are required to evaluate this hypothesis and to determine what factors affect the relationship between microvasculature dropout, and RNFL and GCC thinning in glaucoma.

There has been recent evidence that glaucomatous damage in the macula is detectable in early disease. By including suspects, many with pre-perimetric disease, we provide important documentation of the possible role of microvascular dropout in the macula in early disease. The inclusion of a glaucoma suspect group in this study is important; after adjusting for age, the AUROC curve for differentiating glaucoma suspects and healthy eyes and is greater for wiVD (AUROC=0.705) when compared to GCC thickness (AUC=0.506) ( $P=0.010$ ). Similarly, Yarmohammadi and colleagues reported that ONH wiVD (AUROC=0.70) performed better than RNFL thickness (0.65) when differentiating between glaucoma suspect eyes and healthy eyes.<sup>29</sup> The ability of macula wiVD to outperform GCC thickness in differentiating between glaucoma suspects and healthy eyes may be explained by the previously mentioned possibility that macula vessel density is affected before the retinal nerve fibers. Therefore, macula OCT-A vessel density measurements may be an important adjunctive tool for identifying subjects at risk for developing glaucoma.

Conversely, macula wiVD does not seem to perform better than GCC thickness later in the disease. In the current study, the area under the ROC curve for differentiating glaucoma patients and healthy eyes is greater for GCC thickness (AUC=0.86) when compared to wiVD (AUC=0.76) ( $P=0.011$ ). Other studies have also reported macula GCC presenting a higher AUROC than macula wiVD for differentiating between these 2 diagnostic groups.<sup>60, 61</sup> Both studies had smaller sample sizes compared to the current study. ONH wiVD showed higher but not significantly different diagnostic ability for differentiating between healthy eyes and glaucoma when compared to RNFL thickness (wiVD AUROC=0.94 and RNFL AUROC=0.92<sup>29</sup>; wiVD AUROC=0.84 and RNFL AUROC=0.77<sup>62</sup>). Additional studies that include both macula and ONH OCT and OCT-A imaging should be completed to clarify the role of vessel density compared to thickness measures for differentiating between healthy, glaucoma suspect and glaucoma eyes. It is important to differentiate between what we can detect with a specific instrument and what is the true pathophysiology of the disease. Optical coherence tomography instruments used to measure thickness and OCTA vessel density vary with respect to the scan resolution of scan area. Further studies are therefore needed to determine whether these relationships found in the current study are generalizable to other OCT instruments with a variety of scan sizes and resolutions, or are only found when Angiovue scans of a specific scan resolution and scan size are utilized.



There is consistent evidence from the current study and others that image quality can have an effect on retinal nerve fiber layer thickness using OCT<sup>63, 64</sup> and on OCT-A vessel density measurements.<sup>65</sup> SSI is calculated based on overall signal level (average of backscattered light during acquisition of the entire scan). SSI could be affected by ocular media opacity, corneal surface quality (e.g., tear film), and tissue itself. When there is thinning of the GCC, which is a relatively less bright reflective tissue, overall SSI is lower (personal correspondence with Dr. Qienyuan Zhou, September 2017).

In the current study, the associations between OCT-A SSI and both wiVD and pfVD ( $R^2=53.2\%$  and  $R^2=52.6\%$ , respectively) were strong. Interestingly, OCT-A SSI was not independently associated with MS, MS8 or MS4 in the multivariable analyses. In fact, the strong association between vessel density and OCT-A SSI must be causing multicollinearity. When vessel density is removed from the multiple linear regression analyses, OCT-A SSI is found to be independently associated with 10-2 MS, MS8 and MS4. This is likely because it reflects thinner GCC. In comparison, SD-OCT SSI and GCC thickness show a weaker association ( $R^2=7.8\%$ ). This weaker association may explain why both variables are significantly associated with 10-2 MS independently of each other (Table 5).

IOP was independently and positively associated with 10-2 visual field mean sensitivity (Table 2) because moderate/severe glaucoma subjects had significantly lower IOP as compared to healthy and glaucoma suspects due to intraocular pressure lowering treatment. Thus, in this model, the higher IOP is actually associated with a better visual field mean sensitivity result (higher 1/L value).

The current study has several strengths, including the large sample size, the inclusion of four different diagnostic categories, and the consistent acquisition of all images with the same protocol and using the same instrument. Considering that the relationship between SSI and OCT-A vessel density measurements is strong, SSI should be taken into consideration when comparing results, both cross-sectionally and longitudinally. In the current study, even after adjusting for SSI and other possible confounders in a multivariable analysis of the 10-2 VF MS (Table 2), the significant relationship between the wiVD and central VF test results remained strong.

Several limitations of the current study also should be considered. First, the relatively small scan size (3mm × 3mm) covers an area of the retina that is not as large as the area covered by the 10-2 visual field. This may have affected the strength of the structure-function relationship found, although we also analyzed the mean sensitivity (MS8 and MS4) for the points corresponding to wiVD and pfVD. In addition, the SSI significantly affects the vessel density measurement, and was significantly different among diagnostic groups. For these reasons, we included SSI and age in our multivariable analyses (Tables 2 to 5). It should also be noted that as with thickness measures, there is considerable overlap in the distribution of vessel density in the diagnostic groups. Moreover, as the difference in vessel density among diagnostic groups is generally within previously reported measurement variability the usefulness of vessel density for monitoring progression may be limited<sup>28</sup>. This is due in part due to the large variation in the number of nerve fibers and their axons in the healthy eyes.  
66, 67

In summary, superficial macula vessel density assessed by OCT-A is lower in patients with moderate to severe glaucoma when compared to healthy eyes, glaucoma suspects or mild glaucoma. Further, the wVD and pVD are associated with central 10-2 visual field sensitivities, even after adjusting for SSI. Macula GCC thickness and macula vessel density values are both lower in eyes with mild glaucoma compared to healthy eyes, suggesting that changes of both of these measures are detectable in early disease. Additionally, mean macula vessel density measurements are significantly lower in glaucoma suspects compared to healthy eyes. In contrast, no difference in mean GCC thickness is found when comparing these two diagnostic groups. This suggests that a detectable decrease in macula vessel density precedes detectable macula retinal ganglion cell loss in glaucoma in this study population using the Angiovue instrument. Therefore, macula vessel density is a clinically relevant parameter that may enhance monitoring of glaucoma suspects and patients.

## Acknowledgments

**Funding/Support:** Supported in part by National Institutes of Health/National Eye Institute grants EY011008 (L.M.Z.), EY14267 (L.M.Z.), EY019869 (L.M.Z.), EY027510 (L.M.Z.), core grant P30EY022589; an unrestricted grant from Research to Prevent Blindness (New York, NY); grants for participants' glaucoma medications from Alcon, Allergan, Pfizer, Merck, and Santen. The sponsor or funding organization had no role in the design or conduct of this research.

We thank Felipe Medeiros MD, PhD for biostatistical consultation.

## References

- Weinreb RN, Aung T, Medeiros FA. The pathophysiology and treatment of glaucoma: a review. *JAMA*. 2014; 311(18):1901–11. [PubMed: 24825645]
- Curcio CA, Allen KA. Topography of ganglion cells in human retina. *J Comp Neurol*. 1990; 300(1): 5–25. [PubMed: 2229487]
- Hood DC, Raza AS, de Moraes CG, et al. Glaucomatous damage of the macula. *Prog Retin Eye Res*. 2013; 32:1–21. [PubMed: 22995953]
- Hood DC. Improving our understanding, and detection, of glaucomatous damage: An approach based upon optical coherence tomography (OCT). *Prog Retin Eye Res*. 2017; 57:46–75. [PubMed: 28012881]
- Alhadeff PA, De Moraes CG, Chen M, et al. The Association Between Clinical Features Seen on Fundus Photographs and Glaucomatous Damage Detected on Visual Fields and Optical Coherence Tomography Scans. *J Glaucoma*. 2017; 26(5):498–504. [PubMed: 28333890]
- Kim KE, Kim SH, Oh S, et al. Additive diagnostic role of imaging in glaucoma: optical coherence tomography and retinal nerve fiber layer photography. *Invest Ophthalmol Vis Sci*. 2014; 55(12): 8024–30. [PubMed: 25414196]
- Kim YK, Yoo BW, Jeoung JW, et al. Glaucoma-Diagnostic Ability of Ganglion Cell-Inner Plexiform Layer Thickness Difference Across Temporal Raphe in Highly Myopic Eyes. *Invest Ophthalmol Vis Sci*. 2016; 57(14):5856–63. [PubMed: 27802515]
- Seo JH, Kim TW, Weinreb RN, et al. Detection of localized retinal nerve fiber layer defects with posterior pole asymmetry analysis of spectral domain optical coherence tomography. *Invest Ophthalmol Vis Sci*. 2012; 53(8):4347–53. [PubMed: 22577076]
- Na JH, Kook MS, Lee Y, et al. Detection of macular and circumpapillary structural loss in normal hemifield areas of glaucomatous eyes with localized visual field defects using spectral-domain optical coherence tomography. *Graefes Arch Clin Exp Ophthalmol*. 2012; 250(4):595–602. [PubMed: 22169979]
- Zhang C, Tatham AJ, Abe RY, et al. Macular Ganglion Cell Inner Plexiform Layer Thickness in Glaucomatous Eyes with Localized Retinal Nerve Fiber Layer Defects. *PLoS One*. 2016; 11(8):e0160549. [PubMed: 27537107]

11. Weinreb, RN., Harris, A. Ocular blood flow in glaucoma. Vol. 6. Kugler Publications; 2009.
12. Flammer J, Orgul S, Costa VP, et al. The impact of ocular blood flow in glaucoma. *Prog Retin Eye Res.* 2002; 21(4):359–93. [PubMed: 12150988]
13. Schmidl D, Garhofer G, Schmetterer L. The complex interaction between ocular perfusion pressure and ocular blood flow - relevance for glaucoma. *Exp Eye Res.* 2011; 93(2):141–55. [PubMed: 20868686]
14. Spaide RF, Klancnik JM Jr, Cooney MJ. Retinal vascular layers imaged by fluorescein angiography and optical coherence tomography angiography. *JAMA Ophthalmol.* 2015; 133(1):45–50. [PubMed: 25317632]
15. Jia Y, Morrison JC, Tokayer J, et al. Quantitative OCT angiography of optic nerve head blood flow. *Biomed Opt Express.* 2012; 3(12):3127–37. [PubMed: 23243564]
16. Jia Y, Wei E, Wang X, et al. Optical coherence tomography angiography of optic disc perfusion in glaucoma. *Ophthalmology.* 2014; 121(7):1322–32. [PubMed: 24629312]
17. Shahlaee A, Samara WA, Hsu J, et al. In Vivo Assessment of Macular Vascular Density in Healthy Human Eyes Using Optical Coherence Tomography Angiography. *Am J Ophthalmol.* 2016; 165:39–46. [PubMed: 26921803]
18. Yu J, Jiang C, Wang X, et al. Macular perfusion in healthy Chinese: an optical coherence tomography angiogram study. *Invest Ophthalmol Vis Sci.* 2015; 56(5):3212–7. [PubMed: 26024105]
19. Yarmohammadi A, Zangwill LM, Diniz-Filho A, et al. Relationship between Optical Coherence Tomography Angiography Vessel Density and Severity of Visual Field Loss in Glaucoma. *Ophthalmology.* 2016; 123(12):2498–508. [PubMed: 27726964]
20. Yarmohammadi A, Zangwill LM, Diniz-Filho A, et al. Peripapillary and Macular Vessel Density in Patients with Glaucoma and Single-Hemifield Visual Field Defect. *Ophthalmology.* 2017
21. Sample PA, Girkin CA, Zangwill LM, et al. The African Descent and Glaucoma Evaluation Study (ADAGES): design and baseline data. *Arch Ophthalmol.* 2009; 127(9):1136–45. [PubMed: 19752422]
22. Hodapp, E., Parrish, R., Anderson, D. *Clinical Decisions in Glaucoma.* St Louis, Missouri: CV Mosby Co; 1993. p. 52-61.
23. Racette L, Liebmann JM, Girkin CA, et al. African Descent and Glaucoma Evaluation Study (ADAGES): III. Ancestry differences in visual function in healthy eyes. *Arch Ophthalmol.* 2010; 128(5):551–9. [PubMed: 20457975]
24. Quaranta L, Katsanos A, Russo A, Riva I. 24-hour intraocular pressure and ocular perfusion pressure in glaucoma. *Surv Ophthalmol.* 2013; 58(1):26–41. [PubMed: 23217586]
25. Drasdo N, Millican CL, Katholi CR, Curcio CA. The length of Henle fibers in the human retina and a model of ganglion receptive field density in the visual field. *Vision Res.* 2007; 47(22):2901–11. [PubMed: 17320143]
26. Hood DC, Raza AS. Method for comparing visual field defects to local RNFL and RGC damage seen on frequency domain OCT in patients with glaucoma. *Biomed Opt Express.* 2011; 2(5):1097–105. [PubMed: 21559122]
27. Jia Y, Tan O, Tokayer J, et al. Split-spectrum amplitude-decorrelation angiography with optical coherence tomography. *Opt Express.* 2012; 20(4):4710–25. [PubMed: 22418228]
28. Manalastas PIC, Zangwill LM, Saunders LJ, et al. Reproducibility of Optical Coherence Tomography Angiography Macular and Optic Nerve Head Vascular Density in Glaucoma and Healthy Eyes. *J Glaucoma.* 2017
29. Yarmohammadi A, Zangwill LM, Diniz-Filho A, et al. Optical Coherence Tomography Angiography Vessel Density in Healthy, Glaucoma Suspect, and Glaucoma Eyes. *Invest Ophthalmol Vis Sci.* 2016; 57(9):OCT451–9. [PubMed: 27409505]
30. Sripsema NK, Garcia PM, Bavier RD, et al. Optical Coherence Tomography Angiography Analysis of Perfused Peripapillary Capillaries in Primary Open-Angle Glaucoma and Normal-Tension Glaucoma. *Invest Ophthalmol Vis Sci.* 2016; 57(9):OCT611–OCT20. [PubMed: 27742922]

31. Suh MH, Zangwill LM, Manalastas PI, et al. Deep Retinal Layer Microvasculature Dropout Detected by the Optical Coherence Tomography Angiography in Glaucoma. *Ophthalmology*. 2016; 123(12):2509–18. [PubMed: 27769587]
32. Suh MH, Zangwill LM, Manalastas PI, et al. Optical Coherence Tomography Angiography Vessel Density in Glaucomatous Eyes with Focal Lamina Cribrosa Defects. *Ophthalmology*. 2016; 123(11):2309–17. [PubMed: 27592175]
33. Akagi T, Iida Y, Nakanishi H, et al. Microvascular Density in Glaucomatous Eyes With Hemifield Visual Field Defects: An Optical Coherence Tomography Angiography Study. *Am J Ophthalmol*. 2016; 168:237–49. [PubMed: 27296492]
34. Liu L, Jia Y, Takusagawa HL, et al. Optical Coherence Tomography Angiography of the Peripapillary Retina in Glaucoma. *JAMA Ophthalmol*. 2015; 133(9):1045–52. [PubMed: 26203793]
35. Lee EJ, Lee KM, Lee SH, Kim TW. OCT Angiography of the Peripapillary Retina in Primary Open-Angle Glaucoma. *Invest Ophthalmol Vis Sci*. 2016; 57(14):6265–70. [PubMed: 27849312]
36. Mammo Z, Heisler M, Balaratnasingam C, et al. Quantitative Optical Coherence Tomography Angiography of Radial Peripapillary Capillaries in Glaucoma, Glaucoma Suspect, and Normal Eyes. *Am J Ophthalmol*. 2016; 170:41–9. [PubMed: 27470061]
37. Rao HL, Kadambi SV, Weinreb RN, et al. Diagnostic ability of peripapillary vessel density measurements of optical coherence tomography angiography in primary open-angle and angle-closure glaucoma. *Br J Ophthalmol*. 2016
38. Rao HL, Pradhan ZS, Weinreb RN, et al. Regional Comparisons of Optical Coherence Tomography Angiography Vessel Density in Primary Open-Angle Glaucoma. *Am J Ophthalmol*. 2016; 171:75–83. [PubMed: 27590118]
39. Chihara E, Dimitrova G, Amano H, Chihara T. Discriminatory Power of Superficial Vessel Density and Prelaminar Vascular Flow Index in Eyes With Glaucoma and Ocular Hypertension and Normal Eyes. *Invest Ophthalmol Vis Sci*. 2017; 58(1):690–7. [PubMed: 28134965]
40. Campbell JP, Zhang M, Hwang TS, et al. Detailed Vascular Anatomy of the Human Retina by Projection-Resolved Optical Coherence Tomography Angiography. *Sci Rep*. 2017; 7:42201. [PubMed: 28186181]
41. Iwasaki M, Inomata H. Relation between superficial capillaries and foveal structures in the human retina. *Invest Ophthalmol Vis Sci*. 1986; 27(12):1698–705. [PubMed: 3793399]
42. Rutkowski P, May CA. Nutrition and Vascular Supply of Retinal Ganglion Cells during Human Development. *Front Neurol*. 2016; 7:49. [PubMed: 27092102]
43. Gozlan J, Ingrand P, Lichtwitz O, et al. Retinal microvascular alterations related to diabetes assessed by optical coherence tomography angiography: A cross-sectional analysis. *Medicine (Baltimore)*. 2017; 96(15):e6427. [PubMed: 28403072]
44. Al-Sheikh M, Akil H, Pfau M, Sadda SR. Swept-Source OCT Angiography Imaging of the Foveal Avascular Zone and Macular Capillary Network Density in Diabetic Retinopathy. *Invest Ophthalmol Vis Sci*. 2016; 57(8):3907–13. [PubMed: 27472076]
45. Coscas F, Sellam A, Glacet-Bernard A, et al. Normative Data for Vascular Density in Superficial and Deep Capillary Plexuses of Healthy Adults Assessed by Optical Coherence Tomography Angiography. *Invest Ophthalmol Vis Sci*. 2016; 57(9):OCT211–23. [PubMed: 27409475]
46. Dimitrova G, Chihara E, Takahashi H, et al. Quantitative Retinal Optical Coherence Tomography Angiography in Patients With Diabetes Without Diabetic Retinopathy. *Invest Ophthalmol Vis Sci*. 2017; 58(1):190–6. [PubMed: 28114579]
47. Gadde SG, Anegondi N, Bhanushali D, et al. Quantification of Vessel Density in Retinal Optical Coherence Tomography Angiography Images Using Local Fractal Dimension. *Invest Ophthalmol Vis Sci*. 2016; 57(1):246–52. [PubMed: 26803800]
48. Matsunaga D, Yi J, Puliafito CA, Kashani AH. OCT angiography in healthy human subjects. *Ophthalmic Surg Lasers Imaging Retina*. 2014; 45(6):510–5. [PubMed: 25423629]
49. Li M, Yang Y, Jiang H, et al. Retinal microvascular network and microcirculation assessments in high myopia. *Am J Ophthalmol*. 2016

50. Romano MR, Cennamo G, Schiemer S, et al. Deep and superficial OCT angiography changes after macular peeling: idiopathic vs diabetic epiretinal membranes. *Graefes Arch Clin Exp Ophthalmol*. 2016
51. Samara WA, Shahlaee A, Sridhar J, et al. Quantitative Optical Coherence Tomography Angiography Features and Visual Function in Eyes With Branch Retinal Vein Occlusion. *Am J Ophthalmol*. 2016; 166:76–83. [PubMed: 27038893]
52. Toto L, Borrelli E, Mastropasqua R, et al. Association between outer retinal alterations and microvascular changes in intermediate stage age-related macular degeneration: an optical coherence tomography angiography study. *Br J Ophthalmol*. 2016
53. Toto L, Borrelli E, Mastropasqua R, et al. Macular Features in Retinitis Pigmentosa: Correlations Among Ganglion Cell Complex Thickness, Capillary Density, and Macular Function. *Invest Ophthalmol Vis Sci*. 2016; 57(14):6360–6. [PubMed: 27898981]
54. Wang Q, Chan S, Yang JY, et al. Vascular Density in Retina and Choriocapillaris as Measured by Optical Coherence Tomography Angiography. *Am J Ophthalmol*. 2016; 168:95–109. [PubMed: 27183862]
55. Yang Z, Tatham AJ, Weinreb RN, et al. Diagnostic ability of macular ganglion cell inner plexiform layer measurements in glaucoma using swept source and spectral domain optical coherence tomography. *PLoS One*. 2015; 10(5):e0125957. [PubMed: 25978420]
56. Leite MT, Rao HL, Weinreb RN, et al. Agreement among spectral-domain optical coherence tomography instruments for assessing retinal nerve fiber layer thickness. *Am J Ophthalmol*. 2011; 151(1):85–92e1. [PubMed: 20970108]
57. Chan G, Balaratnasingam C, Yu PK, et al. Quantitative morphometry of perifoveal capillary networks in the human retina. *Invest Ophthalmol Vis Sci*. 2012; 53(9):5502–14. [PubMed: 22815351]
58. Xu H, Yu J, Kong X, et al. Macular microvasculature alterations in patients with primary open-angle glaucoma: A cross-sectional study. *Medicine (Baltimore)*. 2016; 95(33):e4341. [PubMed: 27537559]
59. Shoji T, Zangwill LM, Akagi T, et al. Progressive Macula Vessel Density Loss in Primary Open Angle Glaucoma: A Longitudinal Study. *Am J Ophthalmol*. 2017
60. Chen HS, Liu CH, Wu WC, et al. Optical Coherence Tomography Angiography of the Superficial Microvasculature in the Macular and Peripapillary Areas in Glaucomatous and Healthy Eyes. *Invest Ophthalmol Vis Sci*. 2017; 58(9):3637–45. [PubMed: 28728171]
61. Takusagawa HL, Liu L, Ma KN, et al. Projection-Resolved Optical Coherence Tomography Angiography of Macular Retinal Circulation in Glaucoma. *Ophthalmology*. 2017; 124(11):1589–99. [PubMed: 28676279]
62. Yarmohammadi A, Zangwill LM, Manalastas PIC, et al. Peripapillary and Macular Vessel Density in Patients with Primary Open-Angle Glaucoma and Unilateral Visual Field Loss. *Ophthalmology*. 2017
63. Vizzeri G, Bowd C, Medeiros FA, et al. Effect of signal strength and improper alignment on the variability of stratus optical coherence tomography retinal nerve fiber layer thickness measurements. *Am J Ophthalmol*. 2009; 148(2):249–55e1. [PubMed: 19427621]
64. Balasubramanian M, Bowd C, Vizzeri G, et al. Effect of image quality on tissue thickness measurements obtained with spectral domain-optical coherence tomography. *Opt Express*. 2009; 17(5):4019–36. [PubMed: 19259243]
65. Al-Sheikh M, Ghasemi Falavarjani K, Akil H, Sadda SR. Impact of image quality on OCT angiography based quantitative measurements. *Int J Retina Vitreous*. 2017; 3:13. [PubMed: 28515959]
66. Tan O, Li G, Lu AT, et al. Mapping of macular substructures with optical coherence tomography for glaucoma diagnosis. *Ophthalmology*. 2008; 115(6):949–56. [PubMed: 17981334]
67. Martinez-de-la-Casa JM, Cifuentes-Canorea P, Berrozpe C, et al. Diagnostic ability of macular nerve fiber layer thickness using new segmentation software in glaucoma suspects. *Invest Ophthalmol Vis Sci*. 2014; 55(12):8343–8. [PubMed: 25425301]

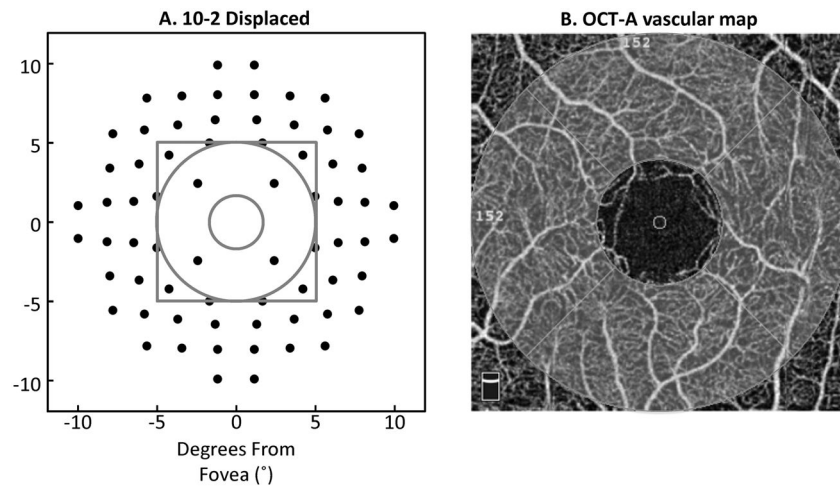


**Figure 1.**

Example of 10-2 visual field with adjustment for retinal ganglion cell displacement, and optical coherence tomography angiography (OCT-A) vascular map. A. The area covered by the 10-2 visual field (black dots) compared with the area covered by the 3mm × 3mm OCT-A scan (gray square). The 4 points inside the gray circle were used for calculation of the mean sensitivity of the 4 central points (MS4), and the 8 points inside the gray square (4 points inside the gray circle included) were used for calculation of the mean sensitivity of the 8 central points (MS8). B. OCT-A vascular map. The whole image vessel density (wiVD) was measured in the entire en-face 3mm × 3mm image, and parafoveal vessel density (pfVD) was measured in an annular region with an inner diameter of 1mm and an outer diameter of 3mm centered on the fovea (in light gray).



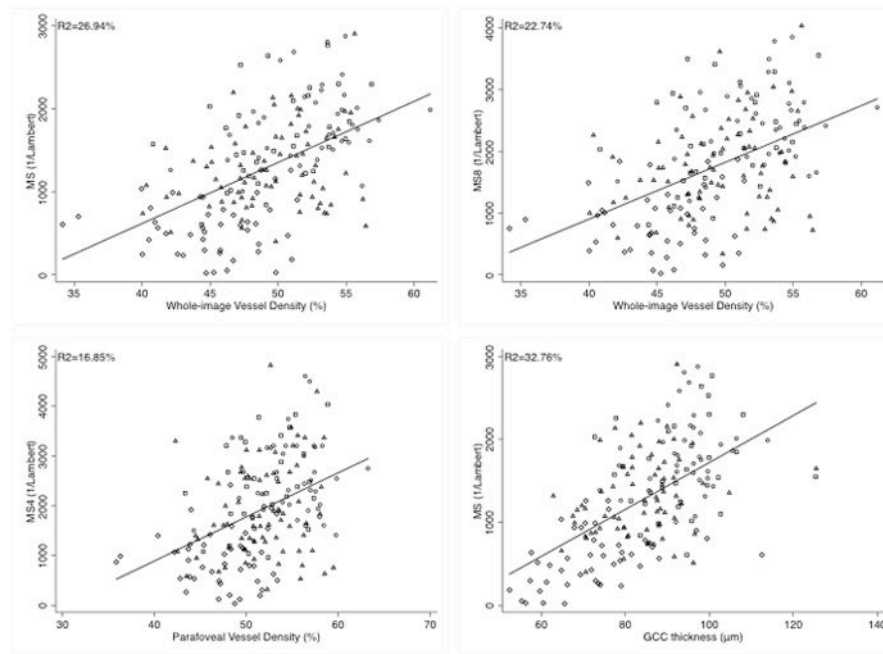


**Figure 2.**

Scatterplots illustrating the linear correlation between: (Top left) the 10-2 standard automated perimetry (SAP) mean sensitivity (MS) and optical coherence tomography angiography (OCT-A) whole image vessel density (wiVD), (Top right) the mean sensitivity of the eight central points (MS8) of the 10-2 and the wiVD, (Bottom left) the mean sensitivity of the four central points (MS4) of the 10-2 and the parafoveal vessel density (pfVD), and (Bottom right) the MS and the ganglion cell complex (GCC) thickness. Healthy, glaucoma suspects, mild glaucoma and moderate to severe glaucoma patients are represented by circles, squares, triangles and diamonds, respectively.

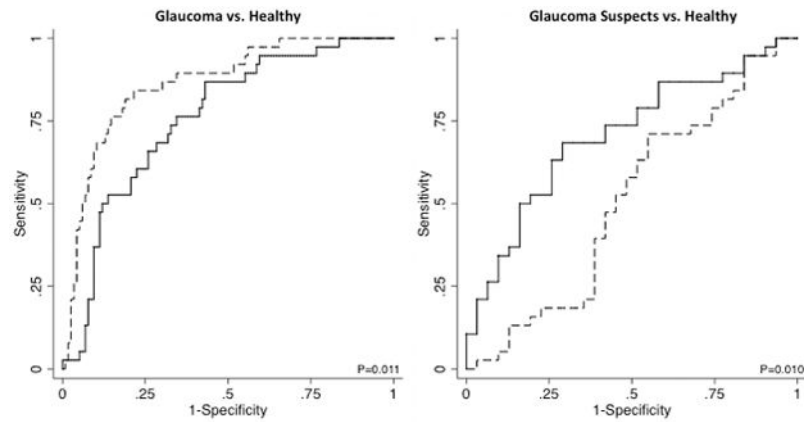


**Figure 3.** Receiver operator characteristic (ROC) curves. (Left) GCC thickness (area under the curve [AUC]=0.863, dashed line) shows better diagnostic ability than macula whole-image vessel density (AUC=0.757, solid line) for differentiating between Glaucoma and Healthy ( $P=0.011$ ). (Right) Macula whole-image vessel density (AUC=0.705, solid line) shows better diagnostic ability than GCC thickness (AUC=0.506, dashed line) for differentiating between Glaucoma Suspects and Healthy ( $P=0.010$ ).

**Table 1**

Demographic and clinical characteristics of subjects included in the study.

Variables	Normal (n = 38)	Glaucoma Suspect (n = 31)	Mild Glaucoma (n = 72)	Moderate/Severe Glaucoma (n = 44)	P-Value
Age, years*	63.8 ± 9.9	67.6 ± 13.2	71.4 ± 9.5	73.9 ± 10.9	<0.001 <sup>‡§¶</sup>
Gender, n (%) females*	28 (73.7)	19 (61.3)	38 (52.8)	17 (38.7)	0.013 <sup>§</sup>
Race, n (%) African-Americans*	13 (34.2)	11 (35.5)	20 (27.8)	8 (18.2)	0.302
MOPP, mmHg*	49.8 ± 7.2	50.3 ± 11.2	50.4 ± 9.1	51.0 ± 9.0	0.949
IOP, mmHg*	15.4 ± 3.0	16.0 ± 4.3	14.0 ± 4.1	12.4 ± 4.4	<0.001 <sup>§¶</sup>
24-2 MD, dB*	0.02 ± 1.16	-0.35 ± 1.28	-2.39 ± 1.90	-13.10 ± 6.59	<0.001 <sup>‡§¶</sup>
10-2 MD, dB*	-0.03 ± 1.07	-0.40 ± 1.26	-2.25 ± 2.83	-12.08 ± 7.10	<0.001 <sup>‡§¶</sup>
OCT-A wIVD, %**	52.5 ± 3.7	49.8 ± 3.7	49.4 ± 3.9	45.2 ± 3.9	<0.001 <sup>‡§¶</sup>
OCT-A pVD, %**	54.9 ± 3.7	52.1 ± 3.7	51.8 ± 4.1	47.7 ± 4.5	<0.001 <sup>‡§¶</sup>
OCT-A SSI**	70.8 ± 7.1	65.9 ± 7.9	66.0 ± 7.0	61.2 ± 7.1	<0.001 <sup>‡§¶</sup>
GCC thickness, μm**	93.9 ± 8.0	93.2 ± 10.7	83.6 ± 10.1	72.5 ± 12.2	<0.001 <sup>‡§¶</sup>
SD-OCT SSI**	70.5 ± 7.4	64.6 ± 10.3	63.7 ± 6.9	59.4 ± 7.8	<0.001 <sup>‡§¶</sup>

dB = decibels; GCC = ganglion cell complex; IOP = intraocular pressure; MD = mean deviation; MOPP = mean ocular perfusion pressure; MS = mean sensitivity; MS4 = mean sensitivity of the four central points; MSS = mean sensitivity of the eight central points; OCT-A = optical coherence tomography angiography; pVD = parafoveal vessel density; SD-OCT = spectral-domain optical coherence tomography; SSI = signal strength index; wIVD = whole-image vessel density

\* Statistical significance tested by ANOVA.

\*\* Statistical significance tested by ANCOVA adjusting for age.

P<0.05 for:

<sup>‡</sup> Healthy vs. Glaucoma suspect,

<sup>‡</sup> Healthy vs. Mild glaucoma,

<sup>§</sup> Healthy vs. Moderate/Severe glaucoma,

<sup>¶</sup> Glaucoma suspect vs. Mild glaucoma,

<sup>¶</sup> Glaucoma suspect vs. Moderate/Severe glaucoma,

<sup>#</sup> Mild glaucoma vs. Moderate/Severe glaucoma.

Multivariable analysis of the relationship between 10-2 visual field mean sensitivity (1/L) and whole image vessel density (wiVD) adjusting for OCT-A SSI, age, gender and IOP.

**Table 2**

Variables	Coefficient	95% CI	P-value
wiVD (per 1% lower)	-39.84	(-66.26 to -13.41)	<b>0.003</b>
Average SSI (per 1 unit lower)	-9.31	(-24.02 to 5.40)	0.213
Age (per 1 year older)	-11.37	(-19.81 to -2.92)	<b>0.009</b>
Gender (Female)	94.54	(-68.75 to 257.82)	0.255
IOP (per 1 mmHg higher)	24.70	(5.51 to 43.90)	<b>0.012</b>

IOP = intraocular pressure; OCT-A = optical coherence tomography angiography; SSI = signal strength index.

Multivariable analysis of the relationship between 10-2 visual field mean sensitivity of the eight central points (1/L) and whole image vessel density (wiVD) adjusting for OCT-A SSI, age, gender and IOP.

**Table 3**

Variables	Coefficient	95% CI	P-value
wiVD (per 1% lower)	-47.62	(-84.79 to -10.47)	<b>0.012</b>
Average SSI (per 1 unit lower)	-9.31	(-30.00 to 11.38)	0.376
Age (per 1 year older)	-17.89	(-29.77 to -6.01)	<b>0.003</b>
Gender (Female)	175.12	(-54.54 to 404.77)	0.134
IOP (per 1 mmHg higher)	24.57	(-2.43 to 51.56)	0.074

IOP = intraocular pressure; OCT-A = optical coherence tomography angiography; SSI = signal strength index.

Multivariable analysis of the relationship between 10-2 visual field mean sensitivity of the four central points (MS4 I/L) and parafoveal vessel density (pfVD) adjusting for OCT-A SSI, age, gender and IOP.

**Table 4**

Variables	Coefficient	95% CI	P-value
pfVD (per 1% lower)	-39.09	(-82.18 to 4.01)	0.075
Average SSI (per 1 unit lower)	-13.60	(-38.51 to 11.31)	0.283
Age (per 1 year older)	-18.80	(-33.12 to -4.49)	<b>0.010</b>
Gender (Female)	200.51	(-77.41 to 478.43)	0.156
IOP (per 1 mmHg higher)	25.39	(-7.21 to 58.00)	0.126

IOP = intraocular pressure; OCT-A = optical coherence tomography angiography; SSI = signal strength index.



Multivariable analysis of the relationship between 10-2 visual field mean sensitivity (1/L) and ganglion cell complex (GCC) thickness adjusting for OCT-A SSI, age, gender and IOP.

**Table 5**

Variables	Coefficient	95% CI	P-value
GCC thickness (per 1 $\mu$ m lower)	-21.58	(-27.18 to -15.98)	<0.001
Average SSI (per 1 unit lower)	-19.41	(-29.74 to -9.07)	<0.001
Age (per 1 year older)	-10.71	(-18.03 to -3.40)	0.004
Gender (Female)	82.49	(-59.88 to 224.87)	0.254
IOP (per 1 mmHg higher)	15.30	(-2.00 to 32.61)	0.083

SSI = signal strength index; SD-OCT = spectral-domain optical coherence tomography; IOP = intraocular pressure.